AN OBSERVATIONAL STUDY OF PROTOPLANETARY CARBON FROM THE GALACTIC CENTER TO THE LOCAL SOLAR NEIGHBORHOOD. Rachel L. Smith[1,2,3], Geoffrey A. Blake[4], A. C. Adwin Boogert[5,6], Klaus M. Pontoppidan[7], Micheal A. Tucker[6], [1]North Carolina Museum of Natural Sciences (rachel.smith@naturalsciences.org), [2]Appalachian State University, Dept. of Physics & Astronomy, [3]UNC Chapel Hill, [4]California Institute of Technology, Div. of Geological & Planetary Sciences,[5]Infrared Telescope Facility, [6]Institute for Astronomy, University of Hawaii, [7]Space Telescope Science Institute.

Introduction: Carbon monoxide (CO) is a valuable tracer of carbon and oxygen chemistry in protoplanetary systems forming across the Galaxy. Large ($\sim$ 8- to 10-m) telescopes enable precise column density derivations from near-IR observations of the CO rovibrational absorption bands; these in turn enable detailed study of protoplanetary chemistry in a range of young stellar environments, and insight into key processes that could have affected the early solar nebula [1-5]. Such observations have explored CO self-shielding [3,5,6], supernova enrichment [4], and interplay between $^{12}C^{16}O$ ice and gas reservoirs [5], primarily toward low-mass YSOs. Massive YSOs are a critical complement to these, as they are bright ($\sim 10^3$ to 10^5 $L_{\rm Sun}$) and can be observed in detail at a greater distance from the Sun. For these targets, precise abundances of gas-phase $^{12}C^{16}O$ and $^{13}C^{16}O$ (heretofore, ^{12}CO, ^{13}CO) isotopologues can be compared to other key carbon reservoirs observed along identical lines of sight, rendering them particularly valuable in evaluating protoplanetary and prebiotic carbon chemistry. Here we present results including our most recent observations from the Keck telescope, extending our study of carbon chemistry from the Galactic center (GC) to the local solar neighborhood ($R_{\rm GC} \sim 8$ kpc).

Observations and Methods: Observations presented here comprise a large survey using NIRSPEC at high-resolution (R$\sim$ 25,000) on the Keck telescope. Our data now include Galactic Center (GC) lines of sight as well as massive YSOs and background stars. Observations thus far span Galactocentric radii ($R_{\rm GC}$) of $\sim$ 0.01 to 9.7 kpc, including the region near SgrA* (the nearest star to the supermassive black hole) and GCS 3 at the GC radio arc, which intercept dense clouds and diffuse ISM near the GC [7]. Target luminosities range from $\sim 1{\times}10^3$ to $\sim 4.7{\times}10^5$ $L_{\rm Sun}$ ($\sim$ 39 $L_{\rm Sun}$ for Elias 29). Fundamental ($v = 1-0$) and first overtone ($v = 2-0$, for optically thin ^{12}CO lines) rovibrational spectra were reduced using our IDL pipeline. Figure 1 shows a portion of the ($v = 1-0$) CO spectrum towards SgrA*, as well as our image of the region taken with Keck-SCAM. We measured equivalent widths (W_ν) of the lines using polynomial + Gaussian fits. For each target, the curve of growth [8] was done in conjunction with a rotational analysis to find the best-fit broadening parameter (b), which in turn was used to derive N_J values for the ^{12}CO and ^{13}CO lines. Total molecular column densities were calculated using b and derived rotational temperatures. The [^{12}CO]/[^{13}CO] were evaluated against other carbon reservoirs for each target.

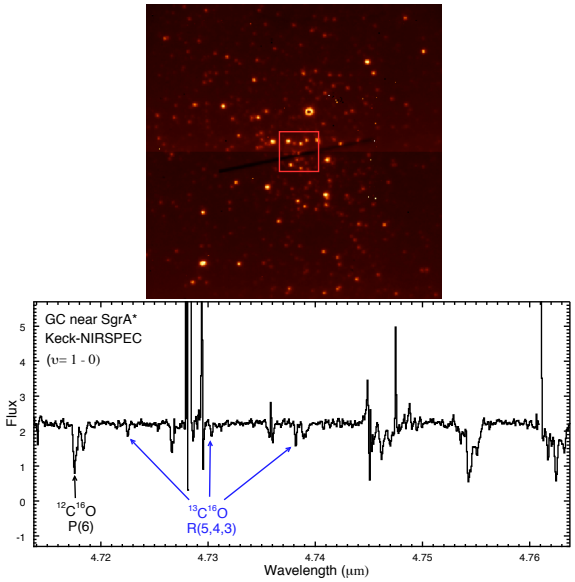

Figure 1: Data for the line of sight toward the region surrounding SgrA*. **Top:** Keck-SCAM image. The boxed region shows the center of the line of sight. **Bottom:** Portion of the CO ($v = 1-0$) rovibrational spectrum taken with Keck-NIRSPEC. Example ^{12}CO and ^{13}CO lines are marked.

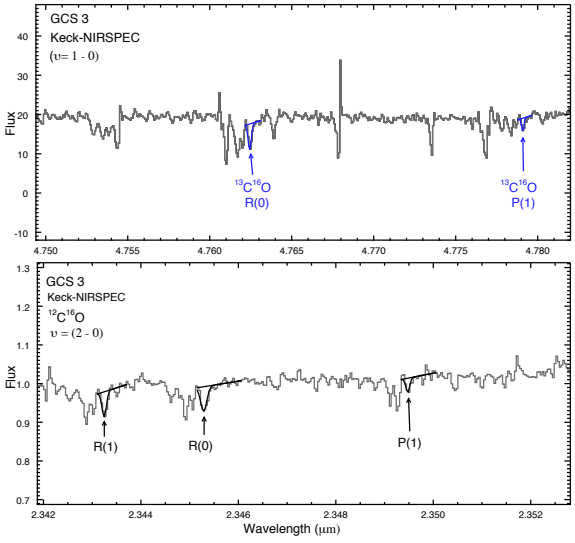

Figure 2: Portions of the rovibrational spectra with line fits for GCS 3, showing observed CO lines. **Top**: Fundamental ($v = 1-0$) band, showing $^{13}C^{16}O$ lines. **Bottom**: First-overtone ($v = 2-0$) band with optically thin $^{12}C^{16}O$ lines.

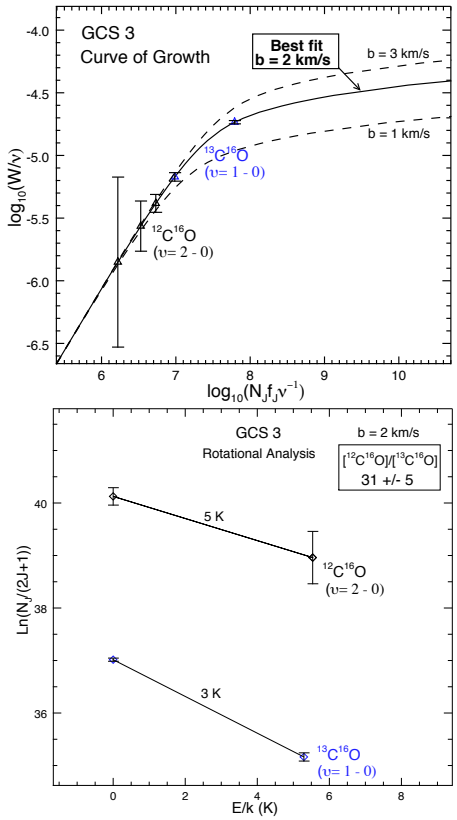

Figure 3: GCS 3 analysis for the five total spectral lines observed. **Top**: Curve of growth showing the best-fit b value (2 km/s), and other comparison velocity curves. **Bottom**: Rotational analysis. Error bars are 1σ, E_J is the energy of the J^{th} rotational state, k is the Boltzmann constant.

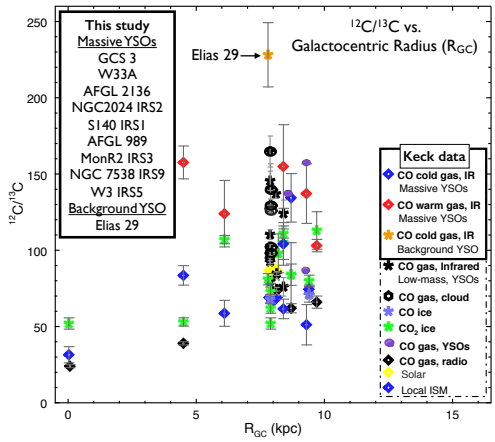

Figure 4: Ratios of $^{12}C/^{13}C$ vs. R_{GC} (kpc) from this study (target names boxed at left, Keck data from this study marked in box at right). Other data: CO gas, Infrared and CO gas, cloud [3,5]; CO ice [10,11]; CO_2 ice [9]; CO gas, (other) YSOs [16]; CO gas, radio [12]; Local ISM [17]; Solar [18].

Results and Discussion: Portions of the $(v = 1 - 0)$ and $(v = 2 - 0)$ spectra for GCS 3 are shown in Figure 2, including line fits. An example curve of growth and rotational plot, here for GCS 3, is shown in Figure 3. Ratios of $[^{12}CO]/[^{13}CO]_{Gas}$ plotted against R_{GC} for analyses thus far are shown in Figure 4. High-resolution $[^{12}CO]/[^{13}CO]_{Gas}$ results for low-mass YSOs ($R_{GC} \sim 8$ kpc) [5], carbon reservoirs of solid CO_2 [9] and CO [10,11], and data from radio observations of $[^{12}C^{18}O]/[^{13}C^{18}O]$ for four of our same lines of sight [12], are also shown. Most of our targets show lower cold-gas-phase $[^{12}CO]/[^{13}CO]$ than $[^{12}CO_2]/[^{13}CO_2]_{Ice}$, suggesting that CO_2 may not derive directly from CO, as assumed [13]. We also find that the cold-gas $[^{12}CO]/[^{13}CO]$ seems to follow a general metallicity trend across the Galaxy, in contrast to the heterogeneity found for low-mass YSOs at $\sim$ 8 kpc [5]. In targets with both warm and cold CO gas, cold-phase $[^{12}CO]/[^{13}CO]$ are lower, similar to what is found for low-mass YSOs [5], suggesting that there may be temperature-dependent CO fractionation pathways that are similar across a range of environments. The very high $[^{12}CO]/[^{13}CO]$ for Elias 29 may be due to its complex radiation and velocity fields [14]. The uniformly lower $[^{12}C^{18}O]/[^{13}C^{18}O]$ from radio observations as compared to our $[^{12}CO]/[^{13}CO]$ for the same lines of sight could be explained by the higher photodissociation rate for $^{12}C^{18}O$ [15].

Conclusions: Our study of protoplanetary carbon across the Galaxy thus far reveals cold CO following a general metallicity trend, while warm CO may undergo different chemical processing in a range of environments. Our results also suggest that CO_2 may not originate from CO. Complex interactions between carbon ice and gas reservoirs, and low- versus high-mass protoplanetary environments, should be included in models exploring carbon chemistry in nebular evolution. The upcoming NIRSPEC resolution upgrade will greatly benefit this ongoing study.

Acknowledgements: We gratefully acknowledge support through NASAs Emerging Worlds Program: (Grant NNX17AE34G [PI, R. Smith]).

References: [1] Brittain S.D. et al. (2005) *ApJ 626*: 283-291. [2] Pontoppidan K. M. (2006) *A&A 453*: L47-L50. [3] Smith R.L. et al. (2009) ApJ 701: 163-179. [4] Young E.D. et al. (2011) *ApJ, 729*: 43-53. [5] Smith R.L. et al. (2015) ApJ *ApJ 813*: 120-135. [6] Lyons J.R. and Young E.D. (2005) *Nature 435, 7040*, 317- 320. [7] Chiar J. E. et al. (2000) *ApJ, 537*: 749-762. [8] Spitzer L. J. (1978) Physical Processes in the Interstellar Medium. [9] Boogert A.C.A. et al. (2000) *A&A 353*, 349-362. [10] Boogert A.C.A et al. (2002) *ApJ 577*, 271-280. [11] Pontoppidan K. M. et al. (2003) *A&A 408*: 981-1007. [12] Langer W.D. and Penzias A. A. (1990) *ApJ 357*, 477-492. [13] van Dishoeck E.F. et al. (1996) *A&A 315*, L349-352. [14] Boogert A.C.A et al. (2002) *ApJ 570* 708-723. [15] van Dishoeck E. F. and Black J. H. (1988) *ApJ 334* 771-802. [16] Goto M. et al. (2003) *ApJ 598*, 1038-1047. [17] Scott P.C. et al. (2006) *A&A. 456*, 675-688. [18] Milam S.N. et al. (2005) *ApJ 634*, 1126-1132.